Shock-induced martensitic transformation of highly oriented graphite to diamond

David J. Erskine and William J. Nellis
Lawrence Livermore National Laboratory, P.O. Box 808, Livermore, California 94550

(Received 9 December 1991; accepted for publication 31 January 1992)

Shock-wave profiles of highly ordered pyrolytic graphite shocked normal to the basal plane of the graphite crystal structure have been measured. For graphite with sufficient orientational order a martensitic transformation to a diamond-like phase is observed with a transition onset pressure 19.6±0.7 GPa, the stability limit of the graphite structure under shock compression. The minimum overpressure required for the transformation is not more than 6 GPa and the two-wave structure of the transition is overdriven to a single wave above 40 GPa.

INTRODUCTION

Because of their great technological importance, the investigation of the carbon phases and how they transform from one to another under pressure is an important field of materials research. A significant part of this research is accomplished using shock waves, since in these experiments uniform and accurately determined pressures can be applied over large sample volumes.

It is well known that diamond is formed by the shock compression of graphite. This process, which occurs in microseconds, happens naturally in the impact of meteors,[1,2] within products of explosives,[3,4] and by explosive compression of powders.[5,6] However, an important issue is whether the shock-induced phase transition of graphite to diamond is martensitic or diffusive. The relation between the crystal structures of graphite and diamond indicates that the phase transition should be fast and martensitic if shock pressure is applied perpendicular to the graphitic basal plane.[7,8] Since the lattice planes of graphite are loosely coupled, small amounts of shear stress naturally existing in the shock state are expected to induce displacive shear motion between the planes so as to produce the diamond stacking sequence.

Recently, several groups have measured the stability of the graphite lattice under *static* compression. Utsumi and Yagi[9] have found that single crystalline graphite begins to transform reversibly to a new phase at 18 GPa, indicated by a sudden increase in the optical transmittance. Takano and Wakatsuki[10] have observed two discontinuous changes in the sample volume with applied load, at 17–18 GPa and 22–23 GPa. Measurements of the pressure dependent Raman spectra by Stishov *et al.*[11] indicate that graphite transforms to a new form above 20 GPa. X-ray diffraction measurements by Hemley *et al.*[12] have found that above 14 GPa graphite transforms to a form with a strength comparable to that of diamond, but with a structure that is neither cubic nor hexagonal diamond. These studies all support the observation that the graphite lattice is unstable above ~20 GPa and that the transformation to the new phase is reversible.

Previous *shock* compression studies of graphite presented an inconsistent picture. A consequence of a martensitic transformation is a well-defined transition onset pressure. Shock studies[13–15] using pressed porous graphite samples indicate a phase transition near 20 GPa, although interpretation of the results is complicated by the heterogeneous temperature distribution due to porosity.[16] In contrast, other studies using pyrolytic graphite (a quasi-single-crystalline form) have observed phase transitions near 34 GPa,[17] 45 GPa,[13] or have failed to see it below 50 GPa.[18] Since pyrolytic samples are more ideal crystalline graphite than porous samples, this wide variety of transformation pressures observed previously seemed inconsistent.

Our preliminary measurements[19] on pyrolytic graphite of two different crystalline grades having different orientational order indicate a strong sensitivity of the transformation on graphite microstructure. Thus we believe the elevated transition pressures observed with pyrolytic samples of earlier studies[13,17,18] were caused by insufficient order in their microstructure, while their high density prevented significant shock heating which could provide a thermally activated transformation.[20] The latter effect likely dominated the behavior of pressed porous samples,[13–15] allowing a transition onset pressure near the crystalline graphite value.

Our studies are the first real-time shock-wave-profile measurements using highly ordered full-density pyrolytic graphite. We report here the shock properties of pyrolytic graphite over a range of pressures, exploring the pressure-volume relation of the compressed diamond-like state, confirming the martensitic nature of the transformation, and refining the value of the transition onset pressure (P_A).

EXPERIMENTAL TECHNIQUE

The locus of states achieved through shock is called a Hugoniot. Because the graphite-diamond transition involves a relatively large volume change, the graphite Hugoniot is expected to have a pronounced kink at the transition onset. This will cause the shock-wave transiting the specimen to bifurcate into two waves,[21] producing a "two-step" structure in the shock pressure and mass velocity profile. This is illustrated in Fig. 1.

For pressures between P_A and P_D the shock occurs in two steps. The first step represents graphite shocked to a state incipient to the transition at a pressure P_A along the

 0021-8979/92/104882-05$04.00 © 1992 American Institute of Physics

Downloaded 28 Feb 2005 to 128.115.175.8. Redistribution subject to AIP license or copyright, see http://jap.aip.org/jap/copyright.jsp

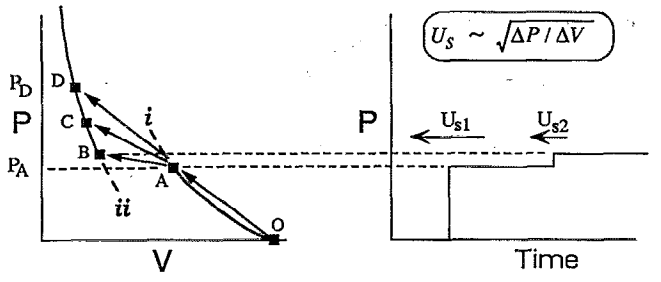

FIG. 1. Illustration of how a system undergoing a phase transition under shock produces a two-step wave-profile. The pressure (P)-volume (V) plot shows the untransformed and transformed graphite Hugoniots i and ii, respectively. The shock OAB produces a stepped wave profile in pressure vs time, and a corresponding one in mass velocity vs time.

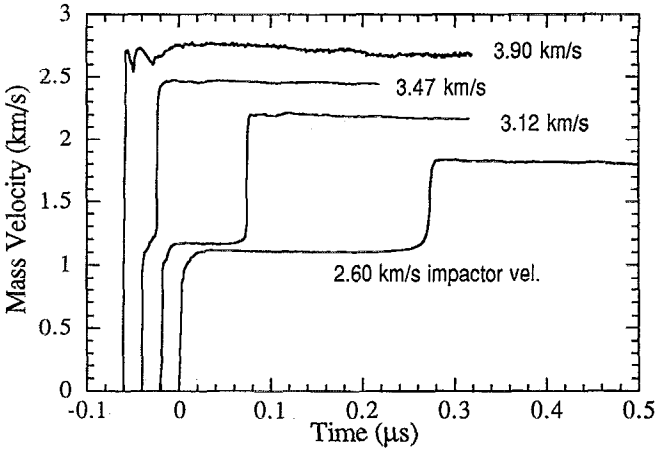

FIG. 3. Wave-profiles of pyrolytic (ZYB) graphite. The curves have been staggered horizontally on the graph for clarity. The two-wave structure is direct evidence for a phase transition.

untransformed Hugoniot i. The second step is a compression into the phase-transformed state represented by Hugoniot ii. The shock speed of the steps (U_{s1},U_{s2}) depends on the slope $\Delta P/\Delta V$ of the jumps in pressure-volume space. As the net shock pressure increases the speed of the second wave approaches the first until there is a single step, when the slope OD exceeds OA (the overdriven condition).

The speed of the phase transition is manifested in the risetime of the second step. If a set of simple displacements exists between two crystal structures the transformation is martensitic and will produce a fast risetime. Thus by measuring the temporal wave-profile we can determine the martensitic nature of the transition and through simple shock relations we can determine the location of the Hugoniot.

Shock-waves were generated by impact of a Cu disk accelerated by a two-stage light-gas gun to velocities of several km/s striking a graphite specimen normal to the basal plane. A schematic of the target is shown in Fig. 2. The specimen was backed by a LiF window through which a laser beam was reflected off the graphite/LiF interface. Since LiF has a shock impedance similar to graphite, the perturbation of the first shock by the interface is relatively small. The laser is the illuminating beam of our VISAR interferometer,[22] which measures mass velocities (U_p) via the Doppler shift of the reflected light with a response time of ~2 ns. Eight electrical shorting pins flush with the front surface of the sample provide a time zero for the start of the shock. The optical/electrical propagation delay of the VISAR is known to ±1 ns so that observation of shock arrival at the sample rear allows shock speed determination to 0.5%. The advantage of our experimental method over other shock diagnostic techniques is that both shock transit times and wave profile amplitudes can be accurately measured. Both these pieces of information are necessary to compute the pressure-volume states achieved during shock-induced phase transformation.

The majority of our samples were highly oriented monochromator grade (ZYB) graphite from Union Carbide measuring 3.5–4 mm thick and 15 mm square. Their densities were 2.254–2.259 g/cm^3, very near the handbook value[23] for crystalline graphite of 2.265 g/cm^3. Several shots were also fired with a lower grade graphite (ZYH) from Union Carbide. This grade is distinguished from the former by beta, the angular width of the (002) x-ray diffraction peak, which measures the spread of misalignment of the crystallite c axes. For the high- and low-grade samples beta is 0.8° and 3.5°, respectively.

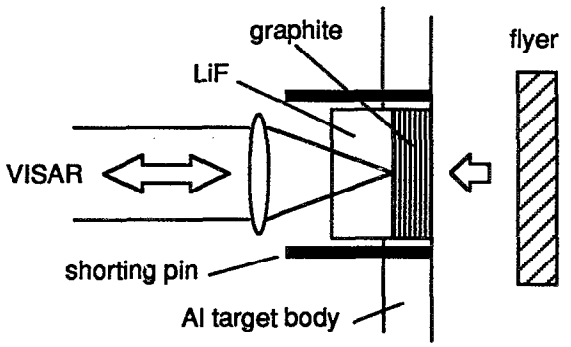

FIG. 2. Target schematic. The VISAR laser beam is Doppler shifted by the movement of the LiF/graphite interface. An interferometer produces a fringe shift proportional to the interface velocity.

WAVE-PROFILE RESULTS

The measured wave-profiles of several shots are shown in Fig. 3. The clean two-step structure demonstrates a martensitic transformation by the rapid (<10 ns) risetime of the second steps. As the impactor speed increases the delay between the steps decreases until a single shock is produced, analogous to the progression OAB, OAC, OAD in Fig. 1. The amplitude of the first step is steady in time, constant from shot to shot, and the second step has a short risetime. Thus this progression of the wave-profile shapes agrees well with the description of a system undergoing a martensitic phase transition for pressures above P_A.

Downloaded 28 Feb 2005 to 128.115.175.8. Redistribution subject to AIP license or copyright, see http://jap.aip.org/jap/copyright.jsp

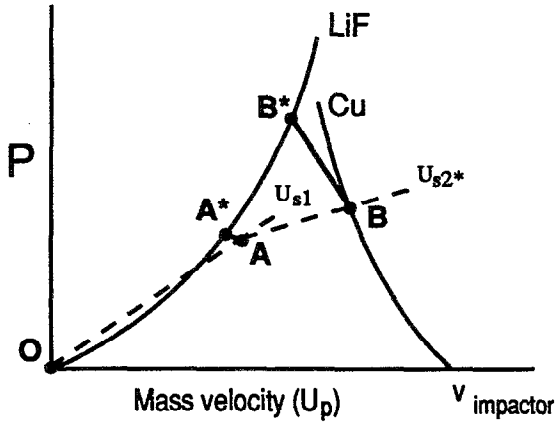

FIG. 4. Construction in pressure (P)-mass velocity (U_p) space for determining compressed states A and B from measured wave profiles. LiF and Cu are Hugoniots of window and impactor. Shock speeds (U_{s1},U_{s2}) of first and second waves determine slopes of OA and OB. The asterisked states represent the first and second waves reflecting off the LiF window.

HUGONIOT DATA ANALYSIS

The wave-profile data was analyzed using standard relations[24] conserving energy, mass, and momentum across the shock front to find the description of the states of graphite during its compression and transformation. The states corresponding to incipient transformation (A), post transformation (B), and reshock off the LiF window (B*) were first found by the construction in pressure-mass velocity space illustrated in Fig. 4 and described below.

We wish to determine states A and B from the measured shock speeds (U_{s1},U_{s2}) and wave-profile amplitudes (U_{pA*},U_{pB*}) of the first and second steps, the impactor velocity, and the known LiF and Cu Hugoniots. The asterisked states A* and B* represent the first and second shock waves reflecting from the LiF window. Since they must lie on the LiF Hugoniot they are determined by the corresponding wave-profile amplitudes U_{pA*} and U_{pB*}. State A must lie on a line from the origin having a slope $\rho_0 U_{s1}$, and its position along that line is determined by the slope of AA*. Since AA* represents a weak compression, we introduce a negligible error in assuming for all shots that the slope of AA* is given by the reflection of line AB found in the lowest pressure shots, or -10 GPa s/km. The second wave propagates as state B, which must lie on the Cu impactor Hugoniot and on a line from A having a slope $\rho_A U'_{s2} = (U_{s2} - U_{pA})/v_A$, where $v_A = (1 - U_{pA}/U_{s1})/\rho_0$. Finally, from U_p, P, and U_s we calculate the specific volume of the states. The relevant measurements and calculation results are tabulated in Tables I and II.

HUGONIOT RESULTS

The shots are plotted in the pressure-volume domain in Fig. 5. Except for the two highest velocity shots which overdrive the transition, a two-step wave-profile exists and there are the following stages of compression: (1) initial shock to transition onset at pressure P_A. This is held until passage of the second wave whereupon there is (2) a rapid transition to the denser phase, and (3) reflection of the second wave off the LiF window. We note that the value of P_A between the four lowest velocity shots is very consistent (19.6 ± 0.7 GPa) compared to the variety of values obtained with the lower grade graphite samples discussed below.

Three shots using the lower grade (ZYH) graphite were performed and the results, shown in Fig. 6 are quite different than with the ZYB grade graphite. In contrast to the sharp transitions seen with the higher grade, the ZYH material shows frustrated transitions, manifested by the elevated and highly variable value of P_A (25–45 GPa), by the finite transition risetime (tens of ns), and by the intermediate states between phases i and ii through which the transformation proceeds.

DISCUSSION

Note that the first and second waves interact differently with the LiF window. Because the Hugoniots of LiF and untransformed graphite are very similar, there is very little reflection of the first wave at that interface. However, when the second wave reaches the window there is a significant reflection and shock-up in pressure. This is because compressed graphite immediately ahead of the second wave is incipient to the phase transition, and therefore much more compressible than the window. Figure 5 shows that the phase transformed graphite has a diamond-like compressibility. This is indicated by the steep slope of the

TABLE I. Measured shot parameters for ZYB graphite. U_{pA*} and U_{pB*} are wave-profile amplitudes behind the first and second steps.

Shot name	Impactor velocity (km/s)	Sample thickness (mm)	Initial density (gm/cm^3)	Two wave speeds (km/s)		Wave-profile amplitude (km/s)	
				U_{s1}	U_{s2}	U_{pA*}	U_{pB*}
gi	4.350	3.448	2.250	ovrdrvn[a]	8.077	ovrdrvn	[b]
gE	3.900	3.977	2.255	ovrdrvn	7.660	ovrdrvn	2.704
gD	3.471	3.862	2.254	7.077	6.922	1.223	2.460
gG	3.120	3.937	2.258	6.966	6.164	1.173	2.202
gF	2.603	3.453	2.255	6.873	4.859	1.110	1.830
g9	2.602	2.463	2.258	6.961	4.727	1.181	1.850
g8	2.605	2.480	2.254	6.931	4.759	1.164	1.812

[a]Overdriven. Only one shock exists.
[b]Wave-profile amplitude was too noisy for a reliable value.

Downloaded 28 Feb 2005 to 128.115.175.8. Redistribution subject to AIP license or copyright, see http://jap.aip.org/jap/copyright.jsp

TABLE II. Compressed states calculated from the wave-profiles described by volume, pressure, and mass velocity.

Shot name	Incipient transition			Post-transition			Reshock of 2nd wave off window	
	v_A (density^{-1})	P_A (GPa)	U_{pA} (km/s)	v_B	P_B	U_{pB}	v_{B^*}	P_{B^*}
gi	ovrdrvn[a]			0.2683	58.20	3.200	[b]	
gE	ovrdrvn			0.2767	49.8	2.880	0.2744	63.30
gD	0.3608	21.1	1.320	0.2782	41.0	2.603	0.2768	55.10
gG	0.3623	19.9	1.267	0.2817	34.7	2.357	0.2798	47.30
gF	0.3660	18.6	1.200	0.2868	26.5	1.992	0.2843	36.90
g9	0.3614	20.1	1.280	0.2876	26.8	1.984	0.2859	37.50
g8	0.3629	19.7	1.261	0.2874	26.7	1.989	0.2842	36.40

[a]Overdriven past the transition.
[b]Wave-profile amplitude was too noisy for a reliable value.

Hugoniot (ii) of second shocked states, as well as the steep slope of the portion of the compression histories corresponding to the reflection of the second wave off the LiF window.

We note that the endpoints of the shock trajectories in Fig. 5 are very reproducibly and consistently falling along a Hugoniot curve (ii) which is distinct from, but parallel to, the diamond Hugoniot.[25] The density of this state is ~5% less than that of diamond for an equivalent pressure. The density difference may be ascribed to thermal pressure and to disorder of hexagonal diamond. Poor crystallization was found in hexagonal diamond recovered from static compression experiments of Bundy.[8] In flash x-ray diffraction measurements during shock compression of pyrolytic graphite, Johnson & Mitchell found that above 20 GPa no well-defined diffraction peaks could be observed, whereas with the same apparatus shocking graphitic BN, well-defined peaks of the phased transformed BN structure were seen.[27]

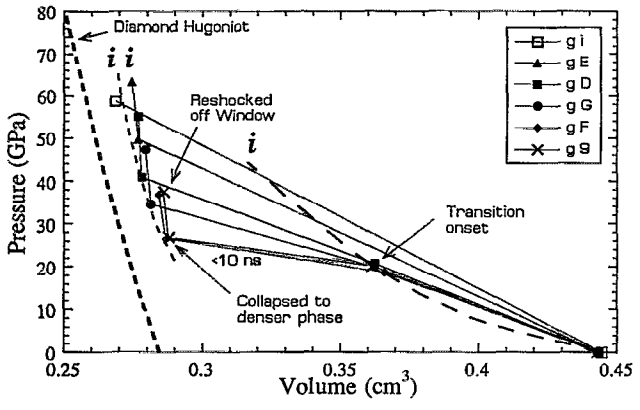

FIG. 5. Pressure-volume histories of high grade (ZYB) pyrolytic graphite. In the two highest velocity shots the transition is overdriven by a single shock which then reflects off the LiF window. In the other shots the shock splits into two waves and the pressure is held at the incipient value P_A until passage of the second wave. Shot g8 was omitted for clarity since it is almost identical to g9. The reflected portion of the data for shot gi was not discernable due to noise. For comparison the measured Hugoniot of diamond (see Ref. 25), and of untransformed graphite (see Refs. 13, 18, and 26) (i) is shown. Curve ii representing the denser phase is a guide for the eyes.

Another possibility is that Hugoniot ii represents a new form of carbon which is distinct from diamond but diamond-like in density and compressibility. A distorted diamond form (*n*-diamond) has recently been recovered in shocked graphite by Hirai and Kondo.[28] The static compression studies[8–12] of graphite support the conclusion that at least one new phase of carbon intermediate in density between graphite and diamond exists. Shu *et al.*[12] indicate that this form has a diamond-like compressibility. That the shock compressed phase is electrically insulating has been determined by Mitchell *et al.*[29] They observed in real time the electrical resistance of pyrolytic graphite shocked to 40 GPa to increase by three orders of magnitude.

The shock temperature in the transformed state is difficult to determine without knowing the cold-compression curve of the diamond-like state. In our previous report[19] we estimated the temperature of this state using preliminary wave-profile data and the cold compression curve of diamond. However, the data in this report imply that the cold-compression curve of the transformed state is significantly different from that of diamond, so that a reliable temperature estimate is not possible.

However, it is possible to calculate the temperature of

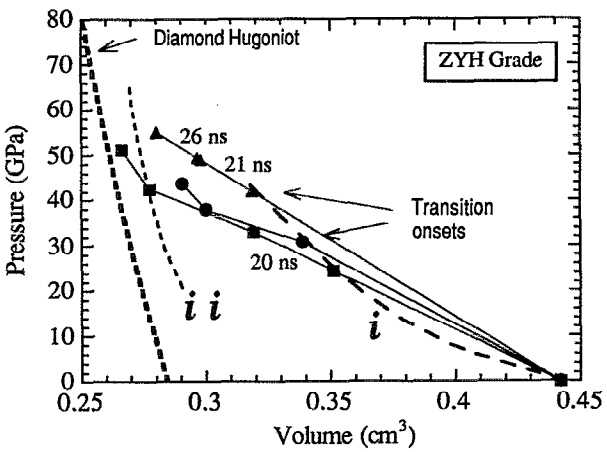

FIG. 6. Pressure-volume histories for the lower grade (ZYH) graphite. As opposed to ZYB grade graphite (Fig. 5), the P_A of this material is highly variable and exceeds 20 GP, and the transition risetimes are significantly longer. Curves i, ii are the same as in Fig. 5.

Downloaded 28 Feb 2005 to 128.115.175.8. Redistribution subject to AIP license or copyright, see http://jap.aip.org/jap/copyright.jsp

graphite at the transition onset. This was calculated to be (500–550 K) by integrating $dT = (V_0 - V)dP/2C_v + [P/2C_v - T\gamma/V]dV$ along the graphite Hugoniot, where $C_v(T)$ is from Ref. 30. The Gruneisen gamma was assumed to range between its graphite and diamond values,[31] $\gamma = 0.35$ and $\gamma = 1.15$, respectively. This temperature is low compared to the melting point[31] of compressed graphite ($\sim$4000 K), and thus supports a martensitic transition rather than a diffusive reconstructive transformation to diamond, which occurs[32] at high shock pressures at 3000–4000 K.

CONCLUSIONS

Our results support a martensitic transformation for highly ordered pyrolytic graphite to a diamond-like state with a 19.6±0.7 GPa transition onset pressure. This pressure represents the stability limit of the graphite lattice to shock loading, and is similar to the $\sim$20 GPa transition onset pressures observed in static compression experiments.[8–13] Martensitic transformations are only observed with graphite of sufficient orientational order. The Hugoniot of the transformed state lies parallel to the diamond Hugoniot (implying diamond-like compressibility), but with $\sim$5% less density. This suggests that the state is a disordered or distorted diamond-like form. The minimum overpressure needed to drive the transition has not been determined, but is as small as 6 GPa. The transition is overdriven above 40 GPa. These experiments illustrate the diagnostic capability that is now available to investigate shock-induced phase transitions in the laboratory.

ACKNOWLEDGMENTS

We acknowledge Ku Moua for fine construction of the targets. This work was performed under the auspices of the U.S. Department of Energy by the Lawrence Livermore National Laboratory under Contract No. W-7405-ENG-48.

[1] R. E. Hanneman, H. M. Strong, and F. P. Bundy, Science **155**, 995 (1967).
[2] R. S. Clarke, D. E. Appleman, and D. R. Ross, Nature **291**, 396 (1981).
[3] N. R. Greiner, D. S. Phillips, J. D. Johnson, and F. Volk, Nature **333**, 440 (1988).
[4] A. I. Lyamkin, E. A. Petrov, A. P. Ershov, G. V. Sakovich, A. M. Staver, and V. M. Titov, Sov. Phys. Dokl. **33**, 705 (1988).
[5] P. S. Decarli and J. C. Jamieson, Science **133**, 1821 (1961).
[6] G. R. Cowan, B. W. Dunnington, and A. H. Holtzman, U.S. Patent No. 3401019, 1968.
[7] S. Fahy, S. G. Louie, and M. L. Cohen, Phys. Rev. B **34**, 1191 (1986); **35**, 7623 (1987).
[8] F. P. Bundy and J. S. Kasper, J. Chem. Phys. **46**, 3437 (1967).
[9] W. Utsumi and T. Yagi, Science **252**, 1542 (1991).
[10] K. J. Takano and M. Wakatsuki, Jpn. J. Appl. Phys. **30**, L860 (1991).
[11] A. F. Goncharov, I. N. Makarenko, and S. M. Stishov, Sov. Phys. JETP **69**, 380 (1989).
[12] J. F. Shu, H. K. Mao, J. Z. Hu, Y. Wu, and R. J. Hemley, Bull. Am. Phys. Soc. II **36**, 479 (1991).
[13] R. G. McQueen and S. P. Marsh, *Behavior of Dense Media Under High Dynamic Pressures* (Gordon and Breech, New York, 1968).
[14] A. V. Anan'in, A. N. Dremin, G. I. Kanel', and S. V. Pershin, Zh. Prikl. Mekh. Tekh. Fiz., No. 3, 112 (1978).
[15] M. F. Gogulya, Fiz. Goreniya. Vzryva **25**, 95 (1989).
[16] R. L. Williamson, J. Appl. Phys. **68**, 1287 (1990).
[17] W. H. Gust, Phys. Rev. B **22**, 4744 (1980).
[18] N. L. Coleburn, J. Chem. Phys. **40**, 71 (1964).
[19] D. J. Erskine and W. J. Nellis, Nature **349**, 317 (1991).
[20] S. V. Pyaternev, S. V. Pershin, and A. N. Dremin, Sov. Combustion, Explosion, and Shock Waves **22**, 756 (1986).
[21] Ya. B. Zeldovich and Yu. P. Raizer, *Physics of Shock Waves and High-Temperature Hydrodynamic Phenomena* (Academic, New York, 1967), pp. 750–756.
[22] W. F. Hemsing, Rev. Sci. Instrum. **50**, 73 (1979).
[23] W. N. Reynolds, *Physical Properties of Graphite* (Elsevier, Amsterdam, 1968), pp. 3–5.
[24] R. G. McQueen, S. P. Marsh, and J. N. Fritz, J. Geophys. Res. **72**, 4999 (1967).
[25] M. N. Pavlovskii, Sov. Phys. Solid State **13**, 741 (1971).
[26] D. G. Doran, J. Appl. Phys. **34**, 844 (1964).
[27] Q. Johnson and A. C. Mitchell, Phys. Rev. Lett. **29**, 1369 (1972).
[28] H. Hirai and K. Kondo, Proc. Jpn. Acad. **67**, 22 (1991); Science **253**, 772 (1991).
[29] A. C. Mitchell, J. W. Shaner, and R. N. Keeler, Physica B **139 & 140**, 386 (1986).
[30] W. C. Morgan, Carbon **10**, 75 (1972).
[31] M. van Thiel and F. H. Ree, Int. J. Thermophys. **10**, 227 (1989).
[32] A. V. Kurdyumov, N. F. Ostrovskaya, and A. N. Pilyankevich, Sov. Powder Metallurgy Metal Ceram. **27**, 32 (1988).

Downloaded 28 Feb 2005 to 128.115.175.8. Redistribution subject to AIP license or copyright, see http://jap.aip.org/jap/copyright.jsp